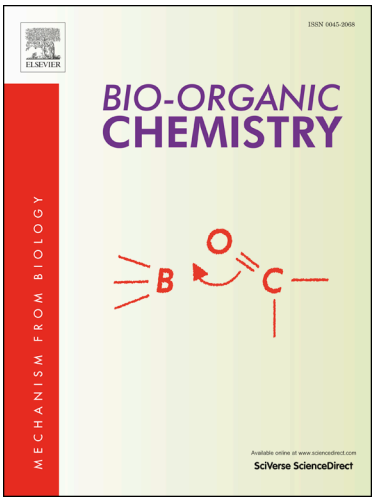

Design and Amberlyst-15 mediated synthesis of novel thienyl-pyrazole carboxamides that potently inhibit Phospholipase A2 by binding to an allosteric site on the enzyme

Achutha Dileep Kumar, Malledevarapura Gurumurthy Prabhudeva, Srinivasan Bharath, Karthik Kumara, Neratur Krishnappagowda Lokanath, Kariyappa Ajay Kumar

PII: S0045-2068(18)30378-X
DOI: https://doi.org/10.1016/j.bioorg.2018.06.023
Reference: YBIOO 2403

To appear in: *Bioorganic Chemistry*

Received Date: 19 April 2018
Revised Date: 14 June 2018
Accepted Date: 18 June 2018

Please cite this article as: A. Dileep Kumar, M. Gurumurthy Prabhudeva, S. Bharath, K. Kumara, N. Krishnappagowda Lokanath, K. Ajay Kumar, Design and Amberlyst-15 mediated synthesis of novel thienyl-pyrazole carboxamides that potently inhibit Phospholipase A2 by binding to an allosteric site on the enzyme, *Bioorganic Chemistry* (2018), doi: https://doi.org/10.1016/j.bioorg.2018.06.023

Design and Amberlyst-15 mediated synthesis of novel thienyl-pyrazole carboxamides that potently inhibit Phospholipase A2 by binding to an allosteric site on the enzyme

Achutha Dileep Kumar,[a] Malledevarapura Gurumurthy Prabhudeva,[a] Srinivasan Bharath,[b] Karthik Kumara,[c] Neratur Krishnappagowda Lokanath,[c] Kariyappa Ajay Kumar[a]*

[a]Department of Chemistry, Yuvaraja College, University of Mysore, Mysuru-570005, India.
[b]Marie Skłodowska-Curie Actions Fellow, Rua da Quinta Grande, 6, 2780-156 Oeiras, Portugal.
[c]Department of Studies in Physics, University of Mysore, Mysuru-570006, India.
*Corresponding author, E-mail: ajaykumar@ycm.uni-mysore.ac.in

Abstract

Inflammation-mediated disorders are on the rise and hence, there is an urgent need for the design and synthesis of new anti-inflammatory drugs with higher affinity and specificity for their potential targets. The current study presents an effective and new protocol for the synthesis of thienyl-pyrazoles through 3+2 annulations using a recyclable heterogeneous catalyst Amberlyst-15. Chalcones **3**(**a-g**) prepared from 3-methylthiophene-2-carbaldehyde and acetophenones by Claisen-Schmidt approach reacted with semicarbazide hydrochloride **4** in the presence of Amberlyst-15 in acetonitrile at room temperature producing thienyl-pyrazole carboxamides **5**(**a-h**) in good yields. Alternatively, the compounds **5**(**a-h**) were prepared by conventional method using acetic acid (30%) medium. Structures of synthesized new pyrazoles were confirmed by spectral and crystallographic studies. All the new compounds were evaluated for their *in vitro* inhibition of Phospholipase A2 from *Vipera russelli* and preliminary studies revealed that, amongst the designed series, compounds **5b**, **5c** and **5h** showed promising inhibition. Further, the compounds exhibited linear mixed-type inhibition behavior for the $sPLA_2$ enzyme indicating that

they bind to an allosteric site distinct from either the calcium or substrate binding site on the enzyme. These kinetic conclusions were further validated by macromolecular rigid-body docking whereby compounds **5c** and **5h** showed binding to distinct pockets on the protein. These findings present a promising series of lead molecules that can serve as prototypes for the treatment of inflammatory related disorders.

Keywords: anti-inflammatory, chalcone, condensation, pyrazole, thiophene.

1. Introduction

Phospholipases A2 (PLA2) are enzymes producing arachidonic acid and lysophospholipids as byproducts of hydrolyzing membrane phospholipids. Subsequently, arachidonic acid and lysophospholipids are metabolized to eicosanoids and platelet-activating factors which play critical roles in the initiation and regulation of inflammation and oxidative stress. Several aberrant neurological conditions are ascribed to inflammation caused by phospholipid metabolism alterations leading to lipid peroxides accumulation and increased phospholipase A2 activities in the brain. Hence, it is essential to design and synthesize novel small-molecule inhibitors for this class of enzymes that can serve as core structures to elaborate for species specific or context-specific inhibition and physiological outcome. Extracts containing natural plant metabolites from curcumin plants, *Centella asiatica* and *Ginkgo Biloba*, have also been extensively assessed as potential inhibitors of phospholipase A2 in cell culture.[1]

Chalcones are the initiators for the biosynthesis of flavonoids and isoflavonoids. Recent reviews on the chalcone derivatives highlights the anti-inflammatory activities, effect of these compounds on lipid peroxidation, heme oxygenase 1(HO-1), cyclooxygenase (COX), and interleukin 5 (IL-5) etc.[2,3] A synthesized series of α,β-unsaturated carbonyl compounds have

showed potent inhibitory activity on $sPLA_2$, cyclooxygenases (COX), soybean lipoxygenase (LOX) in addition to pro-inflammatory cytokines comprising IL-6 and TNF-α.[4,5]

Pyrazoles are an important class of compounds with demonstrated pharmacological properties. A few examples of such properties would include antimicrobial,[6] antioxidant,[7] and anti-inflammatory[8] activities. For instance, synthesized series of pyrazolines have reported to exhibit potent anti- inflammatory related activities such as inhibition of phospholipase A_2 (PLA_2), cyclooxygenases (COX- 1 and COX- 2), IL- 6, and TNF- α.[9] A recent study has also demonstrated by fragment based virtual ligand screening and subsequent experiments that a novel series of pyrazoles can inhibit phospholipase A2, and the most potent inhibitor of the series being 5-(5-isopropyl-2-methylthiophen-3-yl)-1*H* pyrazole 3-carboxamide with IC_{50} of 7.29 µM.[10]

Design and development of an easy procedure for the synthesis of heterocycles with various functionalities that possess wide range of bioactivities with fewer/no side effects is a worthwhile contribution in organic synthesis. A number of synthetic protocols have been reported for the synthesis of pyrazole derivatives in the literature[11-15] etc. However, many of these methods suffer from drawbacks, such as low yields, longer reaction time etc. Thus, development of a facile and eco-friendly method is highly desirable. In recent times, heterogeneous catalysis have played a pivotal role in organic transformations,[16] for example, Amberlyst-15 was found efficient heterogeneous catalyst in the synthesis of quinazolinones.[17] In the present work, we report the use of an inexpensive and reusable catalyst (Amberlyst-15) mediated synthesis of thienyl-pyrazoline carboxamides by the reaction of chalcones with semicarbazide hydrochloride. In order to check the efficiency of the newly employed catalyst, the reaction was carried out by conventional method in acetic acid medium. The synthesized compounds were characterized by

spectral and crystallographic studies, and were evaluated *in vitro* for their inhibition of Phospholipase A2 activities from *Vipera russelli*. The demonstrated synthesis paves the way for future efforts at synthesizing thienyl-pyrazoles that could find widespread applications in bioorganic chemistry.

2. Materials and Methods

Melting points were determined by an open capillary tube method and are uncorrected. Progress of the reactions was checked on thin layer chromatography (TLC) plates pre-coated with silica gel using solvent system hexane**:** ethyl acetate (1:4). The spots were visualized under UV light. ^{1}H NMR and ^{13}C NMR spectra were recorded on Agilent-NMR 400 MHz and 100 MHz spectrometer respectively. Mass spectra were obtained on ESI/APCI-Hybrid Quadrupole, Synapt G2 HDMS ACQUITY UPLC model spectrometer. Elemental analysis was obtained on a Thermo Finnigan Flash EA 1112 CHN analyzer.

2.1 X-Ray diffraction analysis

The compound 3-(2-methoxyphenyl)-5-(3-methylthiophen-2-yl)-4,5-dihydro-1*H*-pyrazole-1-carboxamide **5f** was recrystallized from methanol to give pale yellow crystals suitable for single crystal X-ray diffraction (crystal size 0.23 × 0.34 × 0.27 mm) with the crystallographic parameters: a = 7.681(3) Å, b = 8.346(3) Å, c = 13.149(5) Å, α = 103.609(7)°, β = 103.170(12)°, γ = 97.531(13)°, V = 782.4(5) Å^3, Z = 2, Goodness-of-fit on F^2 = 0.944, R indices (all data) = R1 = 0.1090, wR2 = 0.2150. The complete intensity data sets were processed using *CRYSTAL CLEAR*.[18] The crystal structure was solved by direct method and refined by full-matrix least squares method on F^2 using *SHELXS* and *SHELXL* programs,[19] respectively. The geometrical calculations were performed using *PLATON*.[20] The molecular and packing diagrams were generated using the software *MERCURY*.[21]

2.3 Anti-inflammatory activity

Inflammation is a complex immunological cascade driven by several different factors and can be initiated by manifold cues including, but not limited to, pathogen invasion, tissue damage due to oxidative challenge etc. COX-2 is an important player in bringing about inflammation. Primarily during tissue damage, the first enzyme to get activated is sPLA2, which drives the substrate for COX-2. Inhibition of sPLA2 will result in substrate depletion for COX-2, thereby bringing down the inflammation, as there will be no pro-inflammatory Prostaglandins (PG). In this context, we assessed the inhibitory potential of the synthesized thienyl-pyrazole derivatives, **5**(**a-h**) to inhibit sPLA2, rather than COX-2,[22] This is to ensure that multiple enzyme targets are available for combinatorial drug administration to increase potency and efficacy of blocking the pathway.

2.3.1 Purification of $sPLA_2$ (VRV-PL-8a) from *V. russelli* venom: $sPLA_2$ (VRV-PL-8a) from *Vipera russelli* venom was purified to homogeneity by reported procedure[23] and the protein was estimated by Lowry's method.[24] Briefly, *V. russelli* venom (80 mg) was fractionated on pre-equilibrated Sephadex G-75 column (1.5 × 160 cm) using 50 mM phosphate buffer pH 7.0. The protein was resolved into major three peaks. The second peak, constitute about 30% of the total protein, which showed major $sPLA_2$ activity. This $sPLA_2$ peak fraction was lyophilized and further subjected to pre-equilibrated CM-Sephadex C-25 column (1.5 × 45 cm) chromatography. The fractions were eluted stepwise using phosphate buffers of varied ionic strength (50mM – 200mM) and pH (7.0-8.0). They were resolved into two fractions labeled as V and VIII respectively. The above eluted two fractions were similar to V and VIII protein profiles. The lyophilized fraction VIII was next subjected to Sephadex G-50 column (0.75 ×40 cm)

chromatography and eluted using 50mM phosphate buffer pH 7.0 and obtained peak was checked for sPLA$_2$ activity. Homogeneity was checked by SDS-PAGE and RP-HPLC.

2.3.2 *In vitro* inhibition of VRV-PL-8a by thienyl-pyrazole derivatives, 5(a-h): *In vitro* inhibition of sPLA$_2$ (VRV-PL-8a) by the synthesized pyrazole derivatives, **5(a-h)**, was assessed by the known procedure.[24] Briefly, a 50µl activity buffer containing 50mM Tris-HCl buffer pH 7.5, 10mM $CaCl_2$ and 100µM substrate stock (1mM DMPC in methanol containing 2mM Triton X-100 in Milli-Q water) were added and incubated for 5min at 37ºC. Activity was initiated by adding 10ng of sPLA$_2$ alone or pre incubated with different concentration of thiophene-pyrazole conjugates **5(a-h)** ranging from 0-100µM for 5min at 37°C. Reaction mixtures were incubated for 45min at 37ºC. 50µl of quenching solution was added at a final concentration of 2mM NaN_3, 50µM ANS and 50mM EGTA, vortexed for 30sec and incubated for 5min at rt. 2µL of this solution was pipetted to measure RFU in a Nanodrop ND3300 Ver 2.8 using an excitation UV-LED (370±10nm) and emission was recorded at 480nm in dark condition. Enzyme activity was calculated using the equation

$\Delta RFU = RFU\ (Control) - RFU\ (Test)$

Where, ΔRFU is the change in RFU of test (with sPLA2) with respect to control (without sPLA2) in the presence of inhibitors. The resultant RFU was compared with the standard LPC curve to determine the sPLA2 activity in the presence of inhibitors.

2.3.3 Effect of substrate and calcium concentration on VRV-PL-8a: The effect of substrate and calcium concentration on VRV-PL-8a was estimated by known method.[24] The reaction mixture 0.1ml containing 10mg of sPLA$_2$ alone or with IC_{50} concentration (11.01µM) of inhibitor (test compounds) in 50mM Tris-HCl buffer pH 7.5, 10mM $CaCl_2$ and 10µl of varied substrate stock (0-400µM) was used for sPLA$_2$ assay to check the effect of substrate in presence

of test compounds. 50µl of quenching solution was added at final concentration of 50µM ANS, 2mM NaN_3 and 50mM EGTA, vortexed for 30 sec and incubated for 5 min at RT. 2µl of this solution was pipetted to measure RFU. Similar set of experiment was conducted, where in reaction mixture containing IC_{50} concentration of inhibitor (test compounds) in 50mM Tris-HCl buffer, pH 7.5, 10ng of $sPLA_2$, 100µM substrate and varied concentration of $CaCl_2$ (0-12mM). Reaction was terminated and RFU was measured as described above.

2.3.4 Protein structure quality assessment: The quality of the predicted structure was assessed. Ramachandran plots were generated to understand whether the phi-psi dihedrals are within the allowed regions.[25] Below is the summary of the analysis. As can be seen, the statistics indicates that the structure is reasonably good.

Number of residues in favoured region (~98.0% expected) : 112 (93.3%)
Number of residues in allowed region (~2.0% expected) : 8 (6.7%)
Number of residues in outlier region : 0 (0.0%)
Residue [A 32 :PHE] (-61.55, 105.65) in Allowed region
Residue [A 33 :GLY] (-33.23, -68.80) in Allowed region
Residue [A 39 :TYR] (-143.95, 28.16) in Allowed region
Residue [A 41 :GLY] (47.13,-163.40) in Allowed region
Residue [A 92 :GLY] (-114.18, 59.19) in Allowed region
Residue [A 97 :CYS] (-66.37, -64.58) in Allowed region
Residue [A 129 :PHE] (-74.72, 64.44) in Allowed region
Residue [A 132 :LYS] (-55.19, 174.67) in Allowed region

3. Results

3.1 Synthesis of chalcones, 3(a-h). To a solution mixture of 3-methylthiophene-2-carbaldehyde, **1** (10 mmole) and acetophenones, **2(a-h)** (10 mmole) in methyl alcohol, potassium hydroxide solution (40%, 2 mL) was added. Then the solution mixture was stirred at room

temperature for 2-3 h. The progress of the reaction was monitored by TLC. After the completion, the mixture was cooled to room temperature and poured into ice cold water. The solids separated were filtered, washed successively with cold hydrochloric acid (5%) and cold water. The crude solids were recrystallized from methyl alcohol to obtain compounds **3**(**a-h**).[26]

3.2 Synthesis of pyrazole carboxamides, 5(a-h).

Method A: A mixture of chalcones **5**(**a-h**) (5.0 mmol), semicarbazide hydrochloride **4** (5.0 mmol) and Amberlyst-15 (10%, w/w) in acetonitrile (25 mL) was stirred at room temperature for 30-60 minutes. The progress of the reaction was monitored by TLC. After completion of the reaction, the solid separated was filtered, washed by diethyl ether (2 x 20 mL), dried and treated with EtOAc (20 mL). After stirring for 10 min the mixture was filtered to remove the insoluble catalyst. The filtrate was collected and concentrated under vacuum. The solid isolated was triturated in diethyl ether, filtered and dried to obtain the desired product **5**(**a-h**). The recovered catalyst was washed with EtOAc, dried and reused effectively for four times for a reaction.

Method B: A solution mixture of thiophene based chalcones, **3**(**a-f**) (5 mmole) and semicarbazide hydrochloride, **4** (10 mmole) in acetic acid (30%) was refluxed on a water bath for 1-2 h. The progress of the reaction was monitored by TLC. After the completion, the mixture was filtered and the filtrate was poured into crushed ice. The separated solids were filtered and washed successively with 5% $NaHCO_3$ and water. The crude solids were recrystallized from methyl alcohol to get target molecules **5**(**a-f**) in good yields.

3.2.1 5-(3-Methylthiophen-2-yl)-3-phenyl-4,5-dihydro-1*H*-pyrazole-1-carboxamide, 5a: Obtained from 3-(3-methylthiophen-2-yl)-1-phenylprop-2-en-1-one, **3a** (1.14g, 5 mmole) and semicarbazide hydrochloride, **4** (1.11g, 10 mmole) in 72% yield, m.p. 112-114 °C; ^{1}H NMR ($CDCl_3$, δ ppm): 2.271 (s, 3H, CH_3), 3.196 (dd, 1H, *J=6.9, 16.0Hz*, C_4-H_a), 3.726 (dd, 1H,

J=7.1, 12.6Hz, C_4-H_b), 5.560 (s, 2H, NH_2), 5.745 (dd, 1H, *J=6.9, 12.1Hz*, C_5-H), 6.744 (d, 1H, Ar-H), 7.240-7.641 (m, 6H, Ar-H); ^{13}C NMR ($CDCl_3$, δ ppm): 13.26 (1C, CH_3), 42.60 (1C, C-4), 54.56 (1C, C-5), 120.22 (1C), 122.33 (1C), 124.36 (1C), 128.10 (1C), 128.14 (1C), 128.84 (1C), 128.86 (1C), 133.52 (1C), 130.90 (1C), 135.24 (1C), 151.80 (1C, C-3), 159.87 (1C, C=O). MS *m/z*: 285.09 (M+, 100); Anal. Calcd. for $C_{15}H_{15}N_3OS$ (%): C, 63.13; H, 5.30; N, 14.73; Found: C, 63.01; H, 5.26; N, 14.69.

3.2.2 3-(4-Fluorophenyl)-5-(3-methylthiophen-2-yl)-4,5-dihydro-1*H*-pyrazole-1-carboxamide, 5b: Obtained from 1-(4-fluorophenyl)-3-(3-methylthiophen-2-yl)prop-2-en-1-one, **3b** (1.23g, 5 mmole) and semicarbazide hydrochloride, **4** (1.11g, 10 mmole) in 70% yield, m.p. 104-106 °C; ^{1}H NMR ($CDCl_3$, δ ppm): 2.265 (s, 3H, CH_3), 3.181 (dd, 1H, *J=7.1, 16.6Hz*, C_4-H_a), 3.722 (dd, 1H, *J=7.4, 12.3Hz*, C_4-H_b), 5.554 (s, 2H, NH_2), 5.738 (dd, 1H, *J=6.8, 12.6Hz*, C_5-H), 6.786 (d, 1H, Ar-H), 7.235-7.686 (m, 5H, Ar-H); ^{13}C NMR ($CDCl_3$, δ ppm): 13.35 (1C, CH_3), 45.42 (1C, C-4), 54.40 (1C, C-5), 113.50 (1C), 120.87 (1C), 120.98 (1C), 122.44 (1C), 128.36 (1C), 129.72 (1C), 131.10 (1C), 133.22 (1C), 137.60 (1C), 151.33 (1C, C-3), 153.080 (1C), 159.27 (1C, C=O). MS *m/z*: 303.08 (M+, 100); Anal. Calcd. for $C_{15}H_{14}FN_3OS$ (%): C, 59.39; H, 4.65; N, 13.85; Found: C, 59.30; H, 4.61; N, 13.78.

3.2.3 3-(4-Chlorophenyl)-5-(3-methylthiophen-2-yl)-4,5-dihydro-1*H*-pyrazole-1-carboxamide, 5c: Obtained from 1-(4-chlorophenyl)-3-(3-methylthiophen-2-yl)prop-2-en-1-one, **3c** (1.31g, 5 mmole) and semicarbazide hydrochloride, **4** (1.11g, 10 mmole) in 69% yield, m.p. 114-116 °C; ^{1}H NMR ($CDCl_3$, δ ppm): 2.294 (s, 3H, CH_3), 3.360 (dd, 1H, *J=6.5, 17.0Hz*, C_4-H_a), 3.912 (dd, 1H, *J=6.0, 13.8Hz*, C_4-H_b), 5.687 (s, 2H, NH_2), 5.732 (dd, 1H, *J=6.9, 12.4Hz*, C_5-H), 6.744 (d, 1H, *J=4.0Hz*, Ar-H), 6.970-7.352 (m, 4H, Ar-H), 7.760 (d, 1H, *J=7.3Hz*, Ar-H); ^{13}C NMR ($CDCl_3$, δ ppm): 13.65 (1C, CH_3), 45.50 (1C, C-4), 54.36 (1C, C-5), 120.22 (1C),

121.14 (1C), 121.85 (1C), 128.18 (1C), 128.26 (1C), 129.34 (1C), 129.40 (1C), 133.16 (1C), 134.74 (1C), 137.88 (1C), 151.54 (1C, C-3), 158.27 (1C, C=O). MS *m/z*: 321.05 (M+2, 36.5%), 319.05 (M+, 100); Anal. Calcd. for $C_{15}H_{14}ClN_3OS$ (%): C, 56.33; H, 4.41; N, 13.14; Found: C, 56.21; H, 4.11; N, 13.07.

3.2.4 3-(4-Methoxyphenyl)-5-(3-methylthiophen-2-yl)-4,5-dihydro-1*H*-pyrazole-1-carboxamide, 5d: Obtained from 1-(4-methoxyphenyl)-3-(3-methylthiophen-2-yl)prop-2-en-1-one, **3d** (1.27g, 5 mmole) and semicarbazide hydrochloride, **4** (1.11g, 10 mmole) in 77% yield, m.p. 162-163 °C. ^{1}H NMR ($CDCl_3$, δ ppm): 2.289 (s, 3H, CH_3), 3.356 (dd, 1H, *J=6.9, 17.1Hz*, C_4-H_a), 3.848 (s, 3H, OCH_3), 3.900 (dd, 1H, *J=6.2, 13.2Hz*, C_4-H_b), 5.696 (s, 2H, NH_2), 5.721 (dd, 1H, *J=6.8, 11.9Hz*, C_5-H), 6.731 (d, 1H, *J=4.0Hz*, Ar-H), 6.929-7.365 (m, 4H, Ar-H), 7.853 (d, 1H, *J=7.6Hz*, Ar-H); ^{13}C NMR ($CDCl_3$, δ ppm): 13.90 (1C, CH_3), 45.82 (1C, C-4), 54.45 (1C, C-5), 55.43 (1C, OCH_3), 111.55 (1C), 120.60 (1C), 120.80 (1C), 122.22 (1C), 129.06 (1C), 130.12 (1C), 131.33 (1C), 133.34 (1C), 139.46 (1C), 151.99 (1C, C-3), 155.40 (1C), 158.10 (1C, C=O). MS *m/z*: 315.12 (M+, 100); Anal. Calcd. for $C_{16}H_{17}N_3O_2S$ (%):C, 60.93; H, 5.43; N, 13.32; Found: C, 60.79; H, 5.38; N, 13.22.

3.2.5 3-(3-Methoxyphenyl)-5-(3-methylthiophen-2-yl)-4,5-dihydro-1*H*-pyrazole-1-carboxamide, 5e: The synthesis and characterization was reported earlier.[27]

3.2.6 3-(2-Methoxyphenyl)-5-(3-methylthiophen-2-yl)-4,5-dihydro-1*H*-pyrazole-1-carboxamide, 5f: Obtained from 1-(2-methoxyphenyl)-3-(3-methylthiophen-2-yl)prop-2-en-1-one, **3f** (1.27g, 5 mmole) and semicarbazide hydrochloride, **4** (1.11g, 10 mmole) in 71% yield, m.p. 124-126 °C; ^{1}H NMR ($CDCl_3$, δ ppm): 2.243 (s, 3H, CH_3), 3.189 (dd, 1H, *J=4.8, 17.6Hz*, C_4-H_a), 3.712 (dd, 1H, *J=5.2, 11.2Hz*, C_4-H_b), 3.827 (s, 3H, OCH_3), 5.535 (s, 2H, NH_2), 5.765 (dd, 1H, *J=4.8, 11.6Hz*, C_5-H), 6.730-7.030 (m, 3H, Ar-H), 7.206-7.322 (m, 3H, Ar-H); ^{13}C

NMR ($CDCl_3$, δ ppm): 13.91 (1C, CH_3), 42.71 (1C, C-4), 54.50 (1C, C-5), 55.36 (1C, OCH_3), 111.39 (1C), 116.07 (1C), 119.13 (1C), 122.46 (1C), 129.74 (1C), 130.20 (1C), 132.63 (1C), 133.49 (1C), 139.10 (1C), 151.68 (1C, C-3), 155.26 (1C), 159.76 (1C, C=O). MS *m/z*: 315.10 (M+, 100); Anal. Calcd. for $C_{16}H_{17}N_3O_2S$ (%): C, 60.93; H, 5.43; N, 13.32; Found: C, 60.81; H, 5.40; N, 13.25.

3.2.7 3-(3,4-Dimethoxyphenyl)-5-(3-methylthiophen-2-yl)-4,5-dihydro-1*H*-pyrazole-1-carboxamide, 5g: Obtained from 1-(3,4-dimethoxyphenyl)-3-(3-methylthiophen-2-yl)prop-2-en-1-one, **3g** (1.44g, 5 mmole) and semicarbazide hydrochloride, **4** (1.11g, 10 mmole) in 65% yield, m.p. 130-133 °C. ^{1}H NMR ($CDCl_3$, δ ppm): 2.280 (s, 3H, CH_3), 3.191 (dd, 1H, *J=6.7, 16.4Hz*, C_4-H_a), 3.731 (dd, 1H, *J=6.6, 12.9Hz*, C_4-H_b), 3.848 (s, 6H, OCH_3), 5.556 (s, 2H, NH_2), 5.784 (dd, 1H, *J=6.6, 12.7Hz*, C_5-H), 6.740 (d, 1H, Ar-H), 6.954-6.977 (m, 1H, Ar-H), 7.040-7.346 (m, 3H, Ar-H); ^{13}C NMR ($CDCl_3$, δ ppm): 14.30 (1C, CH_3), 42.82 (1C, C-4), 54.45 (1C, C-5), 55.45 (2C, OCH_3), 111.46 (1C), 114.36 (1C), 121.06 (1C), 121.50 (1C), 122.14 (1C), 125.15 (1C), 127.33 (1C), 133.44 (1C), 150.09 (1C), 151.77 (1C, C-3), 153.26 (1C), 159.90 (1C, C=O). MS *m/z*: 345.11 (M+, 100); Anal. Calcd. for $C_{17}H_{19}N_3O_3S$ (%): C, 59.11; H, 5.54; N, 12.17; Found: C, 59.00; H, 5.49; N, 12.08.

3.2.8 3-(Benzo[d][1,3]dioxol-5-yl)-5-(3-methylthiophen-2-yl)-4,5-dihydro-1H-pyrazole-1-carboxamide, 5h: The synthesis and characterization was reported earlier.[28]

4. Discussion

4.1 Chemistry

Initially, the intermediate 1-(aryl)-3-(3-methylthiophen-2-yl) prop-2-en-1-ones, **3**(**a-h**), were synthesized by base catalyzed reaction of 3-methylthiophene-2-carbaldehyde **1**, with substituted acetophenones, **2**(**a-h**) in methyl alcohol.[26] Then the reaction of **3**(**a-h**) and semicarbazide

hydrochloride **4**, in the presence of heterogeneous catalyst Amberlyst-15 (10%, w/w) in acetonitrile under stirring conditions at room temperature produced thienyl-pyrazole carboxamides, **5**(**a-h**) in good yields. The target compounds, **5**(**a-h**) were also synthesized by conventional method in acetic acid (30%) under reflux conditions, which paves way for understanding the catalytic activity of Amberlyst-15 (**Fig. 1**).

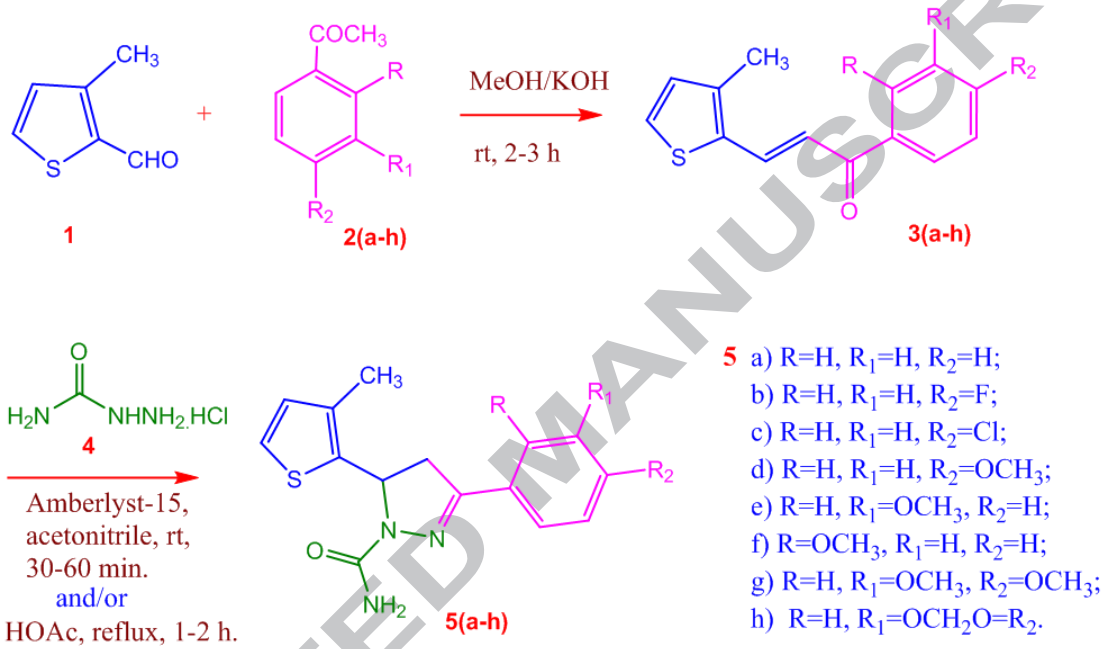

Fig. 1: Synthesis of thienyl-pyrazoline carboxamides, **5**(**a-h**)

The base catalyzed reaction of 3-methylthiophene-2-carbaldehyde **1**, and acetophenones, **2**(**a-h**) in methyl alcohol produced 1-(aryl)-3-(3-methylthiophen-2-yl) prop-2-en-1-one, **3**(**a-h**) in good yields.[26] In search of new potent anti-inflammatory agents, our strategic aim was to synthesize novel thienyl-pyrazole carboxamides. In this context, we carried out the reaction of chalcones **3**(**a-h**) with semicarbazide hydrochloride **4** using recyclable heterogeneous catalyst Amberlyst-15 in acetonitrile at room temperature under stirring conditions to obtain the target compounds thienyl-pyrazole carboxamides, **5**(**a-h**) in good yields. In order to check the efficiency of the catalyst, alternatively the reaction was carried out by conventional method in

acetic acid medium. We observed that, Amberlyst-15 mediated synthesis requires lesser reaction time, and needs no thermal energy in comparison to conventional method in acetic acid; however there was no major difference (±5%) in terms of product yields between the Amberlyte-15 method and the classical method. The Amberlyst-15 catalyst, recovered using the solvent ethyl acetate, was found efficient for four consecutive similar experiments.

^{1}H NMR spectra of compounds **5**(**a-h**) did not show the signals appearing as doublet for each of the alkenyl protons of chalcones **3**(**a-h**), confirming the (3+2) annulations between chalcones and semicarbazide hydrochloride to form the target compounds. Further, the methylene protons of C-4 atom of newly formed pyrazole ring in compounds **5**(**a-h**) exhibited typical ABX spin and were of diastereotopic nature. For instance, in ^{1}H NMR spectrum, the 4-H_a proton of **5f** appeared as doublet of doublet at δ 3.361 (*J=4.8, 17.6Hz*) ppm; whereas, 4-H_b proton appeared as doublet of doublet at δ 3.712 (*J=5.2, 11.2Hz*) ppm, respectively. Instead of appearing as a triplet, 5-H resonates with both 4-H_a and 4-H_b and appears as doublet of doublet at δ 5.765 (*J=4.8, 11.6Hz*) ppm. The singlets appearing at δ 2.243, 3.827 and 5.535 ppm were due to CH_3, OCH_3 and NH_2 protons. Array of signals appearing as multiplets in the region δ 6.730-7.030 and δ 7.206-7.322 ppm were unambiguously assigned to thiophene and aromatic ring protons.

In the ^{13}C NMR spectrum, compound **5f** showed signals at δ 13.91, 55.36 and 159.76 ppm due to CH_3, OCH_3 and C=O carbons. The C-4, C-5 and C-3 carbons of newly formed pyrazole ring showed signals correspondingly at δ 42.71, 54.50 and 151.68 ppm. The appearance of signals for C-4 and C-5 in this region confirms the formation of pyrazoline ring. Aromatic carbons showed the signals in the region δ 111.39-155.26 ppm. In mass spectrum, compound **5f** showed m/z peak at 315.10 corresponding to its molecular mass. All compounds of the

synthesized series **5**(**a-h**) showed similar and consistent pattern signals in their respective spectra and showed satisfactory elemental analyses compared with theoretical values, which strongly favours the formation of the designed products. Further, amongst the series, the structure of **5f** was confirmed by single crystal x-ray diffraction studies. Earlier, we had reported the synthesis, spectral and crystallographic studies of compounds **5e**,[27] and **5h**.[28]

4.2 Crystallography

The molecular structure of the compound 3-(2-methoxyphenyl)-5-(3-methylthiophen-2-yl)-4,5-dihydro-1*H*-pyrazole-1-carboxamide **5f** (CCDC#: **1556966**) was confirmed by single crystal X-ray diffraction analysis. The crystal structure of **5f** is triclinic with a space group of *P-1* and contains pyrazole ring as a central core with three substitutions. Complete crystallographic data refinement details of compound **5f** are given in **Table 1**. The *ORTEP* of the molecule with thermal ellipsoids drawn at 50% probability is shown in **Fig. 2**.

Table 1: Crystal data and structure refinement details of compound **5f**.

Parameter	Value
CCDC deposit No.	CCDC 1556966
Empirical formula	$C_{16}H_{17}N_3O_2S$
Formula weight	315.40
Temperature	293 (2) K
Wavelength	0.71073Å
Crystal system, space group	Triclinic, *P-1*
Unit cell dimensions	a = 7.681(3) Å; b = 8.346(3) Å ; c = 13.149(5) Å α = 103.609(7)^o ; β = 103.170(12)^o ; γ = 97.531(13)^o
Volume	782.4(5) Å^3
Z	2
Density(calculated)	1.339 Mg m $^{-3}$
Absorption coefficient	0.217 mm $^{-1}$
F_{000}	332
Crystal size	0.23 × 0.34 × 0.27 mm

θ range for data collection	3.31° to 27.47°
Index ranges	$-9 \le h \le 6$; $-10 \le k \le 10$; $-17 \le l \le 16$
Reflections collected	4565
Independent reflections	3476 [R int = 0.0664]
Absorption correction	multi-scan
Refinement method	Full matrix least-squares on F^2
Data / restraints / parameters	3476 / 0 / 201
Goodness-of-fit on F 2	0.944
Final [$I > 2\sigma(I)$]	R1 = 0.0630, wR2 = 0.1668
R indices (all data)	R1 = 0.1090, wR2 = 0.2150
Largest diff. peak and hole	0.290 and −0.371 e $Å^{-3}$

Insert Fig.2 here

Fig. 2: *ORTEP* of the molecule **5f** with thermal ellipsoids drawn at 50% probability.

4.3 Anti-inflammatory activity

The results of $sPLA_2$ inhibition studies of synthesized compounds **5(a-h)** are tabulated in **Table 2**. The tested thienyl-pyrazoline carboxamides **5(a-h)**, inhibited $sPLA_2$ in dose depended manner with an IC_{50} value ranging from 9.88 to 36.10 µM. Amongst series, **5c** and **5h** showed significant inhibition against $sPLA_2$ (VRV-PL-8a) with IC_{50} values of 9.88µM and 10.48 µM, respectively, when compared to other structurally related molecules.

Table 2: Neutralization of VRV-PL-8a ($sPLA_2$) by compounds **5(a-h)**[#]

Compound	$sPLA_2$ IC_{50} (µM) ± SEM
5a	14.550 ± 0.132
5b	13.961 ± 0.104
5c*	9.880 ± 0.089
5d	36.108 ± 0.253
5e	25.112 ± 0.220

5f	24.072 ± 0.198
5g	18.446 ± 0.135
5h*	10.482 ± 0.179

*denotes the potent ligand; #Results are expressed as mean ± SEM (n=3).

It has been shown that calcium ions are mandatory for the hydrolysis reaction carried out by $sPLA_2$ by stabilizing the transition state mediated by coordinating the carbonyl group and by shielding the phosphate oxygen's negative charge. Enthalpic interactions contributing to calcium ion binding include conserved aspartic acid residue and carbonyl oxygens of the Tyr and Gly. Thus, to understand the mechanism of action of inhibition and to gain further insight into the sight of binding of the inhibitor vis-à-vis substrate and cofactor, detailed kinetic analysis was undertaken. We carried out the experiments to assess the effect of cofactor calcium ion concentrations (0-12 mM) (**Table 3** and **Fig. 3A-B**) and substrate-1,2-dimyristoyl-sn-glycero-3-phosphocholine (DMPC) concentrations (0-400 µM) (**Table 4** and **Fig. 4C-D**) on $sPLA_2$ (VRV-PL-8a) enzyme inhibition by the compounds **5c** and **5h**. To understand this, compound **5c** and **5h** were kept fixed at their respective IC_{50} concentrations (9.880 µM and 10.482 µM) and the calcium ion was varied from 0-12 mM. **Fig 3A** shows the primary experimental curves fit to Michaelis-Menten equation at no inhibitor and in the presence of **5c** and **5h** respectively.

Table 3: Effect of calcium concentration on $sPLA_2$ (VRV-PL-8a) enzyme inhibition by compounds **5c** (IC_{50} -9.88 µM) and **5h** (IC_{50} -10.48 µM) with varying calcium concentrations (0-12 mM). The results are expressed as mean ± SEM (n=4).

$CaCl_2$ (mM)	$sPLA_2$	$sPLA_2$-**5c**	$sPLA_2$-**5h**
0	0	0	0
1	0.122	0.061	0.060

2	0.165	0.064	0.061
4	0.212	0.098	0.101
6	0.245	0.108	0.124
8	0.290	0.132	0.151
10	0.324	0.150	0.165
12	0.340	0.170	0.190

Table 4: Effect of DMPC concentration (0-400µM) for $sPLA_2$ (VRV-PL-8a) activity in presence of compounds **5c** (IC_{50} -9.88 µM) and **5h** (IC_{50} -10.48 µM). The results are expressed as mean ± SEM (n=4)

DMPC (µ	$sPLA_2$	$sPLA_2$-**5c**	$sPLA_2$-**5h**
0	0	0	0
60	0.720	0.533	0.449
120	0.986	0.660	0.495
180	1.140	0.703	0.580
240	1.244	0.748	0.655
300	1.422	0.789	0.757
360	1.582	0.810	0.828
400	1.652	0.839	0.866

As can be seen from the set of hyperbolic curves, both **5c** and **5h** inhibit the enzyme activity. The nature of inhibition becomes more evident in the double-reciprocal Lineweaver-Burk plots (**Fig. 3B**) whereby both the plots show linear mixed-type inhibition. The Linear regression for **5c** intersects with no inhibitor line in the IIIrd quadrant (indicating increased apparent affinity for calcium of the enzyme leaning towards uncompetitive inhibition) while that for %h intersects in the IInd quadrant (indicating decreased apparent affinity for calcium of the enzyme leaning towards competitive inhibition). However, in both the cases V_{max} of the enzyme decreases indicating unambiguous inhibition. This indicated that the inhibitors bind to allosteric

site different than the calcium binding site and yet modulating calcium binding. However, the experiments would have to be performed at more number of inhibitor concentrations and effects rising due to possible chelation of calcium ions can also be not excluded.

Insert Fig.3 here

Fig. 3: Kinetic analysis of inhibition by **5c** and **5h** on sPLA2 activity **(A)** Non-linear curve fitting of primary calcium titration data **(B)** Double reciprocal Lineaweaver-Burk Plots for calcium titration data. **(C)** Non-linear curve fitting of primary DMPC substrate titration data **(D)** Double reciprocal Lineaweaver-Burk Plots for DMPC substrate titration data

The results of substrate DMPC titrations indicated the same behavior as seen for calcium ion (**Fig 3C** and **Fig 3D**) possibly suggesting that the binding site of these compounds are distal than the cofactor and substrate binding site and inhibitor binding can either facilitate substrate binding (for **5c**) or inhibit substrate binding (for **5h**) to $sPLA_2$ (VRV-PL-8a) However, as has been pointed out above, the experiments would have to be performed at more number of inhibitor concentrations to enable global nonlinear model fifing and rigorous assessment mechanism.

4.4 Protein modelling, Ligand-similarity metrics and Docking studies

There are several structures available for Basic phospholipase A2 VRV-PL-VIIIa from *Vipera russelii* in the PDB database (UNIPROT ID: P59071). As a first step, we used these structures for docking studies. However, the results from the above docking analysis prevented us from assessing the translational potential of these small-molecules as potential intervention agents for human anti-inflammatory purposes and to compare and contrast the results with the pyrazole inhibitor reported for human phospholipase A2 (see below for detailed). The aim of the current exercise was to model a soluble phospholipase A2 with closest similarity to the human

homologue. Thus, the protein modelling was performed as follows. The sequence of the human soluble phospholipase A2 (PDB id: 5G3M) was queried to search for similar sequences in the *D. russelii* genome that resulted in acidic phospholipase A2 (A8CG87.1) from *D. russelii* as the closest hit (43 % sequence identity and e-value of 3e-26).[29] This protein sequence was modelled on the template 1oz6 with 68.33 % sequence coverage (Global model quality estimate of 0.76). The quality control parameters of the predicted structure were assessed[25] and are as specified in **Fig. 4**.

Insert Fig.4 here

Fig. 4: Ramachandran plot of all the residues (left panel) and of general, glycine, proline and preproline-proline residues (right panel).

Before carrying out detailed docking analysis of the small-molecule with modelled structure, we wanted to understand possible pharmacophore similarity across the small-molecules synthesized and their similarity with the closest reported small-molecule inhibitor of soluble phospholipase A_2 reported in literature 5-(5-isopropyl-2-methylthiophen-3-yl)-1*H* pyrazole 3-carboxamide.[9]

Table 5: Comparison of the synthesized molecules by rigid-body and flexible superposition done using LS-align.[30]

Mol	Ref	Rigid superposition				Flexible superposition			
		PC Score[1]	PC Score[2]	Jaccard Ratio	$RMSD_{LS}$	PC Score[1]	PC Score[2]	Jaccard Ratio	$RMSD_{LS}$
5a (20)	5c (21)	0.9991 (2.7 × 10^{-5})	0.9515 (5.7 × 10^{-5})	0.9524	0.1800	0.9991 (2.7 × 10^{-5})	0.9515 (5.7 × 10^{-5})	0.9524	0.1800
5b (21)	5c (21)	0.9965 (2.9 × 10^{-5})	0.9965 (2.9 × 10^{-5})	1.0000	0.0000	0.9965 (2.9 × 10^{-5})	0.9965 (2.9 × 10^{-5})	1.0000	0.0000
5c (21)	5c (21)	1.0000 (2.8 × 10^{-5})	1.0000 (2.8 × 10^{-5})	1.0000	0.0000	1.0000 (2.8 × 10^{-5})	1.0000 (2.8 × 10^{-5})	1.0000	0.0000
5d	5c	0.9407 (7.6 × 10^{-5})	0.9855 (3.7 × 10^{-5})	0.9545	0.1759	0.9407 (7.6 × 10^{-5})	0.9855 (3.7 × 10^{-5})	0.9545	0.1759

(22)	(21)								
5e (22)	5c (21)	0.8872 (1.82×10^{-4})	0.9295 (9.2×10^{-5})	0.7917	0.4122	0.8879 (1.8×10^{-4})	0.9301 (9.1×10^{-5})	0.7917	0.5377
5f (22)	5c (21)	0.8637 (2.67×10^{-4})	0.9048 (1.38×10^{-4})	0.6538	0.3885	0.8646 (2.63×10^{-4})	0.9058 (1.36×10^{-4})	0.7200	0.5063
5g (24)	5c (21)	0.8616 (3.1×10^{-4})	0.9846 (4.2×10^{-5})	0.8750	0.3766	0.8616 (3.1×10^{-4})	0.9846 (4.2×10^{-5})	0.8750	0.3766
5h (23)	5c (21)	0.8758 (2.32×10^{-4})	0.9592 (6.0×10^{-5})	0.9130	0.2717	0.8758 (2.32×10^{-4})	0.9592 (6.0×10^{-5})	0.9130	0.2717
Ref[3] (17)	5c (21)	0.3637 (0.399462)	0.2944 (0.775864)	0.0000	102.5398	0.3637 (0.399462)	0.2944 (0.775864)	0.0000	102.5398

[1]is if normalized by atom number of Query Ligand, [2] is if normalized by atom number of template Ligand

As can be understood from **Table** 5, the best hit **5c** resembles **5b** the closest and distantly resembles **5e** among the ensemble of synthesized compounds. However, compound **5c** shares no similarity, whatsoever, with the only know pyrazole compound 5-(5-isopropyl-2-methylthiophen-3-yl)-1*H* pyrazole 3-carboxamide that has been shown to possess activity against $sPLA_2$ enzyme.[9] This observation enhances the importance of the current work and demonstrates its novelty.

The obtained high quality model was used to perform *in silico* docking experiments with the small-molecules **5c** and **5h** that showed the most potent IC-50 values for phospholipase A2 inhibition. Docking analysis with **5b** was not performed because of its high similarity to **5c**. SWISS-DOCK was used to perform the docking with the calcium bound structure. Explicit hydrogens were added to the ligands employing OpenBabel,[31] and the structures were minimized with Chimera. **Table 6** summarizes the docking parameters of the top hits for molecule **5c** and **5h**.

Table 6: Summary of the docking parameters for the top pose of small molecules **5c** and **5h**

Ligand	Receptor	Full Fitness (kcal/mol)	Estimated ΔG (kcal/mol)
5c	Model 1	-737.55	-8.34
5h	Model 1	-744.66	-8.28

Perusal of **Fig. 5**(**A-D**) for the top binding clusters of **5c** and **5h** point to the fact that they bind to two distinct allosteric pockets. **Fig. 5 A-B** shows the top ten poses of the molecule **5c** and **5h** and **Fig. 5C-D** shows the surface representation depicting the depth of the pocket accommodating **5c** and **5h,** respectively. As is observed from the figure, the top poses of the small-molecules **5c** and **5h** with low binding energies (-8 to -7 kcal/mol) all cluster compactly (< 1 Å root mean square deviation) within the predicted docking pocket. It has to be pointed out that the two distinct pockets to which **5c** and **5h** bind, are different than either the substrate binding or the cofactor binding pockets.

Insert Fig.5 here

Fig. 5: Determination of the site of binding for 5c and 5h. Ribbon representation of the protein with top ten docked poses of the small-molecules in ball and stick representation for **(A) 5c** and **(B) 5h**. To emphasize the binding pocket, surface representation of the protein with small-molecules in ball and stick representation for **(C) 5c** and **(D) 5h**

Careful analysis of the top most poses belonging to cluster 1 for **5h** indicates that all of them bind to a highly conserved pocket on the protein's surface that corresponds exactly to the pocket in which the only know pyrazole compound 5-(5-isopropyl-2-methylthiophen-3-yl)-1*H* pyrazole 3-carboxamide, which has inhibitory activity on $sPLA_2$ enzyme, binds (PDB ID: 4UY1)[9] (**Fig. 6A**). This could explain the distinct inhibition kinetics observed for this compound vis-à-vis calcium and substrate DMPC. Just to emphasize, compound **5h** shows an inhibition

pattern with both calcium and DMPC which resembles a linear mixed-type inhibition whereby binding of inhibitor makes the enzyme lose both its activity and affinity for the substrate/cofactor.

Insert Fig.6 here

Fig. 6: Superposition of 4uy1 (purple) with pyrazole ligand TJM (red) (5-(2,5-dimethyl-3-thienyl)-1h-pyrazole-3-carboxamide) with **(A)** the modeled structure docked with **5c** and the **(B)** modeled structure docked with **5h**. Calcium ion is shown as sphere (orange).

However, the top poses belonging to cluster 1 for **5c** binds to a completely novel, yet unreported, pocket (**Fig. 6B**). To the best of our knowledge, this is the first report demonstrating the utilization of this allosteric pocket by a novel pyrazole family of compounds to inhibit the enzyme. To reiterate the inhibition mechanism shown by this compound, and to find plausible rationalization from the docking pose, it would have to be pointed out that compound **5c** shows an inhibition pattern with both calcium and DMPC which resembles a linear mixed-type inhibition whereby binding of inhibitor makes the enzyme lose its activity but gain increased affinity for the substrate/cofactor.

The structural insights into the site of binding and the nature of interactions for **5c** and **5h** shows that the latter binds to a conserved pocket that is shared by an already reported pyrazole compound. However, the allosteric site to which **5c** binds is very novel and unique and paves the way for a lot of future investigation that would enable the design of better inhibitors for phospholipase A2 with better geometrical and charge complementarities with the pocket and resultant increase in its affinity and potency.

Conclusions

In the present work, we developed a new procedure for the synthesis of thiophene-pyrazole conjugates from various thienyl chalcones using a recyclable Amberlyst-15 catalyst. The method is a simple and reliable approach towards the synthesis of pyrazoles, Amberlyst-15 was developed as new efficient reusable heterogeneous catalyst for the synthesis of pyrazole derivatives. Synthesized compounds were characterized by spectral and crystallographic studies. *In vitro* studies on anti-inflammatory activity of the synthesized compounds, **5(a-h)** shows that; amongst the series, compounds **5c**, and **5h** exhibit excellent VRV-PL-8a inhibition activities. The thienyl, chlorophenyl and methylenedioxyphenyl substitution on pyrazole ring is posited to be the key feature for the biological potency of the synthesized compounds. The results of the study pave way for the development of new anti-inflammatory drugs.

Conflict of Interest: All authors no conflict of interest including financial, personal or other relationships with other people or organizations for this article.

Acknowledgments

The authors are grateful to the IOE Instrumentation Facility, Vijnana Bhavana, University of Mysore, for recording spectra and x-ray diffraction studies.

References

[1] W.-Y. Ong, T. Farooqui, G. Kokotos, A.A. Farooqui, Synthetic and natural inhibitors of phospholipase A2: their importance for understanding and treatment of neurological disorders. ACS Chem. Neurosci. 6 (2015) 814–831.

[2] S.N.A. Bukhari, M. Jasmai, I. Jantan, Synthesis and biological evaluation of chalcone derivatives (Mini Review), Mini Rev. Med. Chem. 12 (2012) 1394-1403.

[3] S.N.A. Bukhari, I. Jantan, M. Jasmai, Anti-inflammatory trends of 1, 3-diphenyl-2-propen-1-one derivatives, Mini Rev. Med. Chem. 13 (2013) 87-94.

[4] S.N.A. Bukhari, G. Lauro, I. Jantan, G. Bifulco, M.W. Amjad, Pharmacological evaluation and docking studies of α,β-unsaturated carbonyl based synthetic compounds as inhibitors of secretory phospholipase A_2, cyclooxygenases, lipoxygenase and proinflammatory cytokines, Bioorg. Med. Chem. 22 (2014) 4151-4161.

[5] I. Jantan, S.N.A. Bukhari, O.A. Adekoya, I. Sylte, Studies of synthetic chalcone derivatives as potential inhibitors of secretory phospholipase A2, cyclooxygenases, lipoxygenase and pro-inflammatory cytokines, Drug Des. Dev. & Therapy, 8 (2014) 1405-1418.

[6] M. Govindaraju, G. Vasanth Kumar, B.N. Mylarappa, K. Ajay Kumar, Synthesis of 8-(5-aryl-4-octyl-2-phenyl-3,4-dihydro-2*H*-pyrazol-3-yl)-octanoic acid ethyl esters via 1, 3-dipolar cycloaddition reaction, IOSR J. App. Chem. 2 (2012) 1-4. DOI: 10.9790/5736-0210104.

[7] R. Nagamallu, B. Srinivasan, M.B. Ningappa, A.K. Kariyappa, Synthesis of novel coumarin appended bis(formylpyrazole) derivatives: Studies on their antimicrobial and oxidant activities, Bioorg. Med. Chem. Lett. 26, (2016) 690-694.

[8] Z. Sui, J. Guan, M.P. Ferro, K. McCoy, M.P. Wachter, W.V. Murray, M. Singer, M. Steber, D.M. Ritchie, D.C. Argentieri, 1,3-Diarylcycloalkanopyrazoles and diphenyl hydrazides as selective inhibitors of cyclooxygenase-2, Bioorg. Med. Chem. Lett. 10 (2000) 601–604.

[9] S.N.A. Bukhari, X. Zhang, I. Jantan, H.-L. Zhu, M.W. Amjad, V.H. Masand, Synthesis, molecular modeling, and biological evaluation of novel 1, 3- diphenyl- 2- propen- 1- one based pyrazolines as anti- inflammatory agents, Chem. Biol. Drug Des. 85 (2014) 729-742.

[10] H. Chen, L. Knerr, T. Akerud, K. Hallberg, L. Oster, M. Rohman, K. Osterlund, H.G. Beisel, T. Olsson, J. Brengdhal, J. Sandmark, C. Bodin, Discovery of a novel pyrazole series of group X secreted phospholipase A2 inhibitor (sPLA2X) via fragment based virtual screening, Bioorg. Med. Chem. Lett. 24 (2014) 5251-5255.

[11] F.S. Al-Saleh, I.K. Al Khawaja, J.A. Joule, Synthesis of 4-acyl- and 4-alkoxy-carbonylpyrazoles, J. Chem. Soc. Perkin Trans. 1 (1981) 642–645.

[12] A. Barakat, N. Shivalingegowda, N. Renuka, A.K. Kariyappa, M. Abdoh, I. Warad, N.K. Lokanath, Crystal structure of 3-(thiophene-2-yl)-5-p-tolyl-4,5-dihydro-1*H*-pyrazole-1-carboxamide, Zeitschrift fur Kryst.-New Cryst. Str. 231 (2016) 267-269.

[13] K. Mohanan, A.R. Martin, L. Toupet, M. Smietana, J.-J. Vasseur, Three-component reaction using the bestmann–ohira reagent: a regioselective synthesis of phosphonyl pyrazole ring, Angew. Chem. Int. Ed. 49 (2010) 3196–3199.

[14] N. Renuka, A.K. Kariyappa, Synthesis and biological evaluation of novel formyl-pyrazoles bearing coumarin moiety as potent antimicrobial and antioxidant agents, Bioorg. Med. Chem. Lett. 23 (2013) 6406-6409.

[15] J. Prabhashankar, V.K. Govindappa, A.K. Kariyappa, Synthesis of 3,4-diaryl-1-phenyl-4,5-dihydro-1*H*-pyrazole-5-carbonitriles via 1,3-dipolar cycloaddition reactions. Turk. J. Chem. 37 (2013) 853-857.

[16] S. Park, K.M. Cho, M.H. Youn, J.G. Seo, S.H. Baeck, T.J. Kim, Y.M. Chung, S.H. Oh, I.K. Song, Epoxidation of propylene with hydrogen peroxide over TS-1 catalyst synthesized in the presence of polystyrene, Cat. Lett. 122 (2008) 349-353.

[17] P.V.N.S. Murthy, D. Rambabu, G.R. Krishna, C.M. Reddy, K.R.S. Prasad, M.V.B. Rao, M. Pal, Amberlyst-15 mediated synthesis of 2-substituted 2,3-dihydroquinazolin-4(1H)-ones and their crystal structure analysis, Tetrahedron Lett. 53 (2012) 863–867.

[18] Rigaku, *CRYSTAL CLEAR*, Rigaku Corporation, Tokyo, Japan, (2011).

[19] Sheldrick, G.M. Crystal structure refinement with SHELXL, Acta Crystallography Section C, Structural Chemistry, 71 (2015) 3−8.

[20] A. L. Spek, *PLATON* An integrated tool for the analysis of the results of a single crystal structure determination, Acta Cryst. A46 (1990) C34–C34.

[21] C.F. Macrae, I. J. Bruno, J. A Chisholm, P.R. Edgington, P. McCabe, E. Pidcock, L. Rodriguez-Monge, R. Taylor, J. van de Streek, P.A. Wood, CSD 2.0 - New features for the visualization and investigation of crystal structures, J. Appl. Cryst. 41 (2008) 466–470.

[22] D.M. Lokeshwari, N.D. Rekha, B. Srinivasan, H.K. Vivek, A.K. Kariyappa, Design, synthesis of novel furan appended benzothiazepine derivatives and *in vitro* biological evaluation as potent VRV-PL-8a and H^+/K^+ ATPase inhibitors, Bioorg. Med. Chem. Lett. 27 (2017) 3048-3054.

[23] S. Kasturi, T.V. Gowda, Purification and characterization of a major phospholipase A2 from Russell's viper (Vipera russelli) venom, Toxicon, 27 (1989) 229-237.

[24] D.M. Lokeshwari, D.K. Achutha, B. Srinivasan, N. Shivalingegowda, L.N. Krishnappagowda, A.K. Kariyappa, Synthesis of novel pyrazole analogues with potent affinity anti-inflammatory effect mediated by inhibition of phospholipase A2: Crystallographic, *in silico* docking and QSAR analysis. Bioorg. Med. Chem. Lett. 27 (2017) 3806-3811.

[25] S.C. Lovell, I.W. Davis, W.B. Arendall III, P.I.W. de Bakker, J.M. Word, M.G. Prisant, J.S. Richardson, D.C. Richardson, Structure validation by Calpha geometry: phi,psi and Cbeta deviation, Proteins: Str. Funct. & Genetics, 50 (2002) 437-450.

[26] M.G. Prabhudeva, K. Kumara, A.D. Kumar, M.B. Ningappa, N.K. Lokanath, K.A. Kumar, Amberlyst-15 catalyzed synthesis of novel thiophene–pyrazoline derivatives: spectral and crystallographic characterization and anti-inflammatory and antimicrobial evaluation, Res. Chem. Intermed. (2018). DOI: 10.1007/s11164-018-3501-2.

[27] K. Kumara, A.D. Kumar, K.A. Kumar, N.K. Lokanath, Synthesis, spectral and X-ray crystal structure of 3-(3-methoxyphenyl)-5-(3-methylthiophen-2-yl)-4,5-dihydro-1H-pyrazole-1-carboxamide: Hirshfeld surface, DFT calculations and thermo-optical studies, Chem. Data Coll. 13-14 (2018) 40-59.

[28] K. Kumara, A.D. Kumar, S. Naveen, K.A. Kumar, N.K. Lokanath, Synthesis, spectral characterization and X-ray crystal structure studies of 3-(benzo[d][1,3]dioxol-5-yl)-5-(3-methylthiophen-2-yl)-4,5-dihydro-1*H*-pyrazole-1-carboxamide: Hirshfeld surface, DFT and thermal analysis, J. Mol. Str. 1161 (2018) 285-298.

[29] M.G. Prabhudeva, S. Bharath, A.D. Kumar, S. Naveen, N.K. Lokanath, B.N. Mylarappa, K.A. Kumar, Design and environmentally benign synthesis of novel thiophene appended pyrazole derivatives as anti-inflammatory and radical scavenging agents: crystallographic, *in silico* modeling, docking and SAR characterization, Bioorg. Chem. 73 (2017) 109-120.

[30] J. Hu, Z. Liu, D.J. Yu, Y. Zhang, LS-align: an atom-level, flexible ligand structural alignment algorithm for high-throughput virtual screening, Bioinfomatics, (2018) doi: 10.1093/bioinformatics/bty081.

[31] N.M. O'Boyle, M. Banck, C.A. James, C. Morley, T. Vandermeersch, G.R. Hutchison, Open Babel: An open chemical toolbox, J. Cheminf. 3 (2011) 33. DOI: 10.1186/1758-2946-3-33.

Graphical abstract

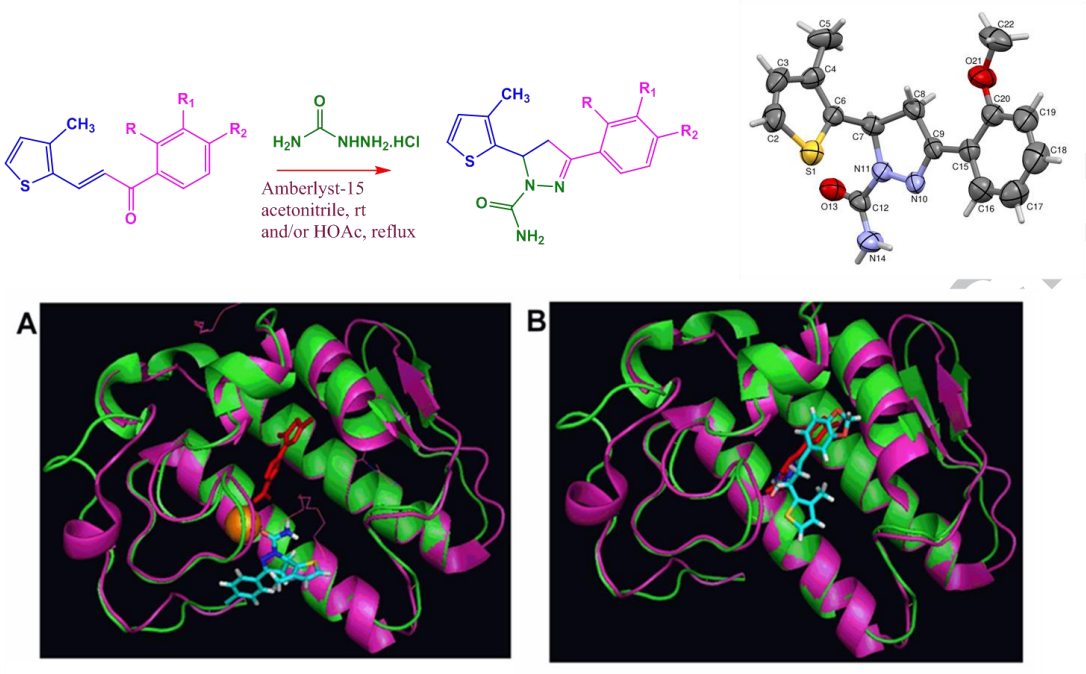

Highlights (mandatory)

- Amberlyst-15 has been developed as new efficient catalyst for the synthesis of pyrazoline derivatives. Alternatively the synthesis of pyrazole analogues was carried out in acetic acid (30%) medium.
- The synthesized pyrazoles have potently inhibited Phospholipase A2 by binding to an allosteric site on the enzyme.
- Structures of three target molecules have confirmed by spectroscopic and crystallographic studies.
- *in silico* modeling, docking and SAR characterization provides insights into the molecular features conferring potency